

# Analytical description of three-dimensional reachable set for Dubins car

*Patsko V.S., Fedotov A.A.*



*Krasovskii Institute of Mathematics and Mechanics,  
Ural Branch of RAS, Ekaterinburg, Russia*



**The 61st Israel Annual Conference on Aerospace Sciences,**  
March 9 – 10, 2022

## Slide 1

We work at the N.N.Krasovskii Institute of Mathematics and Mechanics, Yekaterinburg, Russia. The photo shows the central entrance to our Institute. Our report is devoted to the three-dimensional reachable set for the “Dubins car” model, namely, to the analytical description of the reachable set. “Reachable set” and “reachability set” are synonyms for us.

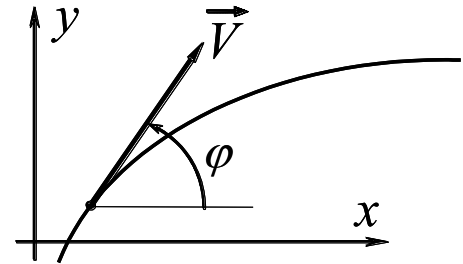
# Dubins Car

$$\dot{x} = \cos \varphi, \quad u_1 = -1 \quad (\text{symmetric case})$$

$$\dot{y} = \sin \varphi, \quad u_1 \in (-1, 0) \quad (\text{asymmetric case})$$

$$\dot{\varphi} = u; \quad u_1 = 0 \quad (\text{one-sided turn case})$$

$$u \in [u_1, 1]. \quad u_1 \in (0, 1) \quad (\text{strictly one-sided turn case})$$



$$\varphi \in (-\infty, +\infty)$$

The model "Dubins car" is used to approximate the dynamics of various controlled objects

**A.A. Markov (1889), R. Isaacs (1951), L. Dubins (1957)**

*E. J. Cockayne, G. W. C. Hall, T. Pecsvaradi, Yu. I. Berdyshev, A.W. Merz, J.-P. Laumond, P. Souères, H.J. Sussmann, S.M. LaValle, T. Shima, M. Weiss, Z. Chen, G. Merkulov, P. Tsiotras, E. Bakolas, M. Pachter, R. Murphey, H. Choi, C.Y. Kaya, M. Vendittelli, D. Casbeer, E. Garcia, M. Mitchell, C.J. Tomlin, M.E. Buzikov, A.A. Galyaev, S. Cacace, A.S. Matveev, A.V. Savkin, Yu.L. Sachkov, A.A. Ardentov, R. Takei, R. Tsai, N.D. Botkin, V.L. Turova, V.N. Ushakov, A.T. Becker, ...*

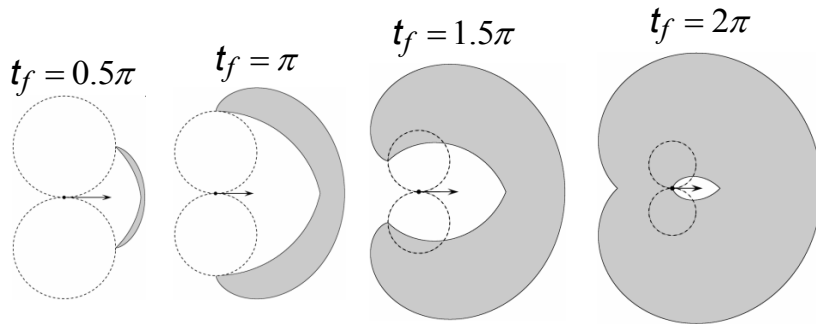
## Slide 2

Here, the standard kinematic description of the "Dubins car" is shown. With respect to the left value in the specification of the constraint on the control  $u$ , we distinguish 4 cases: symmetric case, asymmetric case, one-sided turn case, and strictly one-sided turn case. In our report, we will talk only about the symmetric case. The angular coordinate  $\varphi$  changes in the interval  $(-\infty, \infty)$ .

Of course, there are a lot of works in the modern literature related to the analysis of the Dubins car model (or those close to it) and to using it in solving various control problems or even game problems. We give a far from complete list of authors of publications on this topic.

First of all, we mention A.A.Markov, R.Isaacs, and L.Dubins.

# Reachable set in projection onto a geometric plane $x, y$



SIAM J. CONTROL  
Vol. 13, No. 1, January 1975

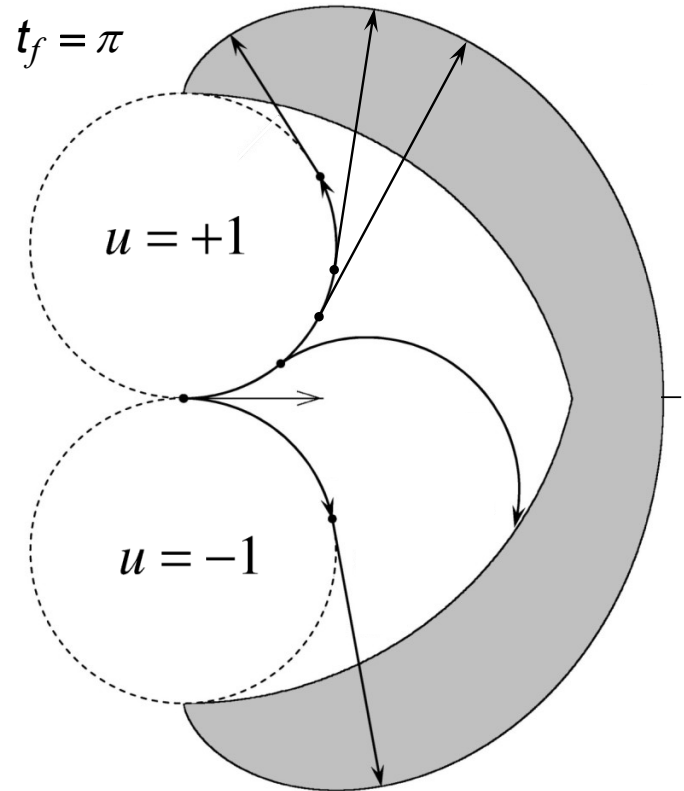
## PLANE MOTION OF A PARTICLE SUBJECT TO CURVATURE CONSTRAINTS\*

E. J. COCKAYNE AND G. W. C. HALL†

**Abstract.** A particle  $P$  moves in the plane with constant speed and subject to an upper bound on the curvature of its path. This paper studies the classes of trajectories by which  $P$  can reach a given point in a given direction and obtains, for all  $t$ , the set  $R(t)$  of all possible positions for  $P$  at time  $t$ , thus extending the results of several recent authors.

Yu.I.Berdyshev

Nonlinear Problems in Sequential Control and Their Application  
Ekaterinburg: IMM UB RAS, 2015, 193 p. (in Russian)



*The boundary consists of two involutes of a circle (the frontal part) and two cardioids (the rear part)*

## Slide 3

In the remarkable paper by E.J. Cockayne and G.W.C. Hall, an analytical description of the reachable set for the Dubins car in geometric coordinates  $x, y$  is given and the evolution of the reachable set in time is studied. The frontal part of the reachable set boundary is a smooth junction of two involutes, the rear part of the boundary is composed of two cardioids with non-smooth joining.

At our Institute, Yu.I. Berdyshev also worked with the reachable set in geometric coordinates in the early 70s. Six years ago, he published a book presenting his results on solving various control problems using the Dubins model and its generalizations.

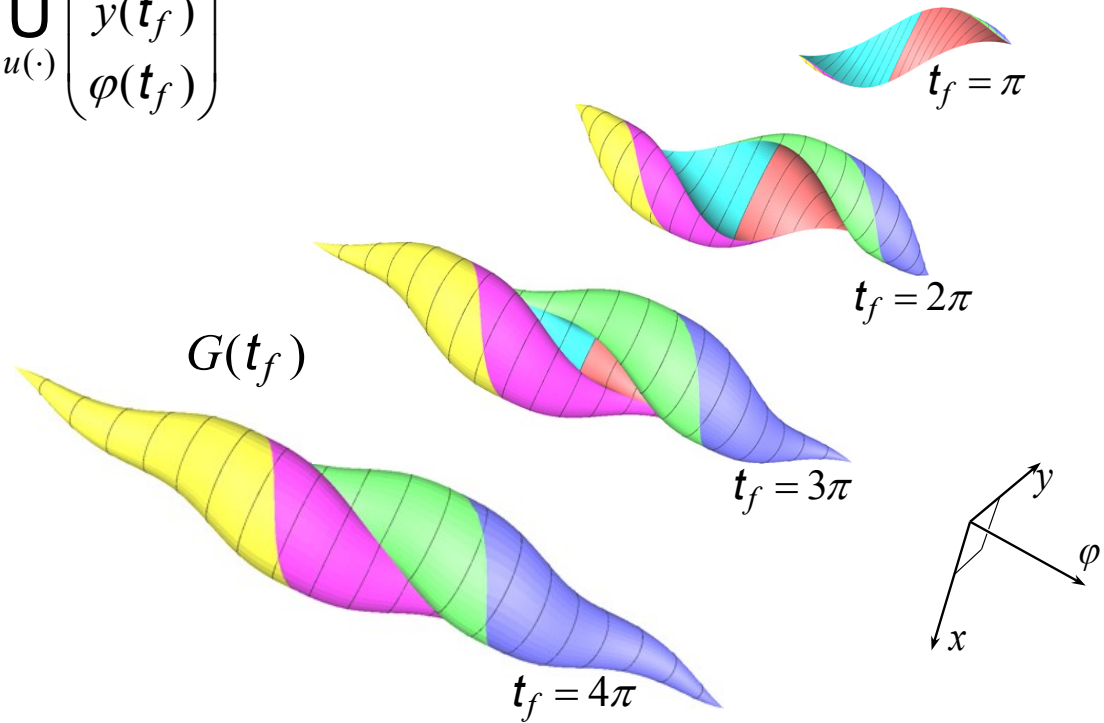
We emphasize that the reachable set in the geometric coordinates  $x, y$  is the projection of the three-dimensional reachable set (which is constructed in the coordinates  $x, y, \varphi$ ) onto the two-dimensional plane  $x, y$ .

# Three-dimensional reachable set “at the instant”

$$G(t_f) = \bigcup_{u(\cdot)} \begin{pmatrix} x(t_f) \\ y(t_f) \\ \varphi(t_f) \end{pmatrix}$$

$$t_0 = 0, \quad x(t_0) = y(t_0) = \varphi(t_0) = 0$$

- (+1, 0, +1)
- (-1, 0, +1)
- (+1, 0, -1)
- (-1, 0, -1)
- (+1, -1, +1)
- (-1, +1, -1)



$G_\varphi(t_f)$  is a  $\varphi$ -section

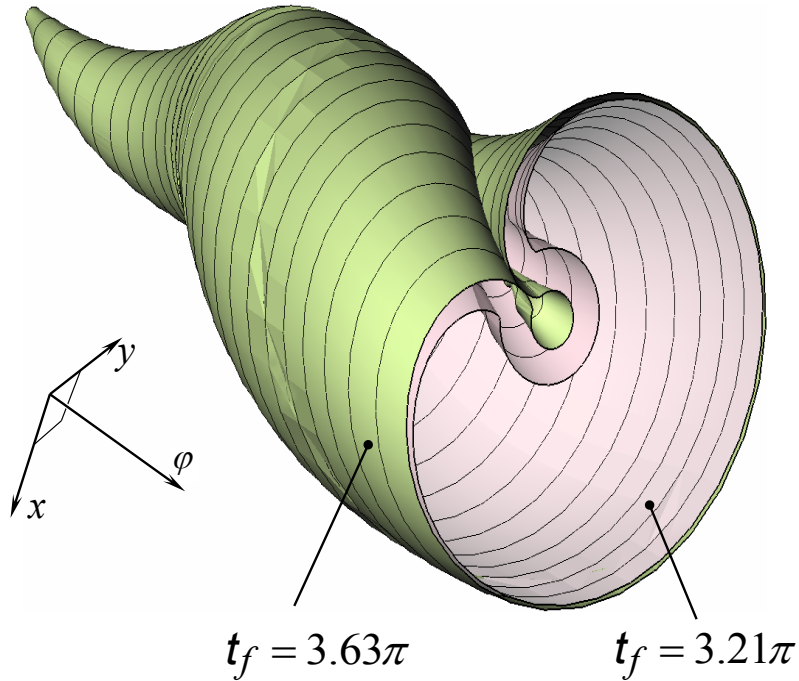
## Slide 4

This slide represents the time evolution of the three-dimensional reachable set for the Dubins car. Recall that we consider the reachable set “at the instant”. It is the union of all three-dimensional phase states at a fixed time  $t_f$ , each of which can be reached with the help of some admissible control.

The figure shows the results of numerical constructions taken from our 2003 paper. To construct the boundary of the reachable set, it is sufficient to use six control types with no more than two switchings. The symbol  $G_\varphi(t_f)$  will denote the two-dimensional  $\varphi$ -section of the three-dimensional set  $G(t_f)$  by the angular coordinate  $\varphi$ . Namely, these  $\varphi$ -sections will be interesting for us.

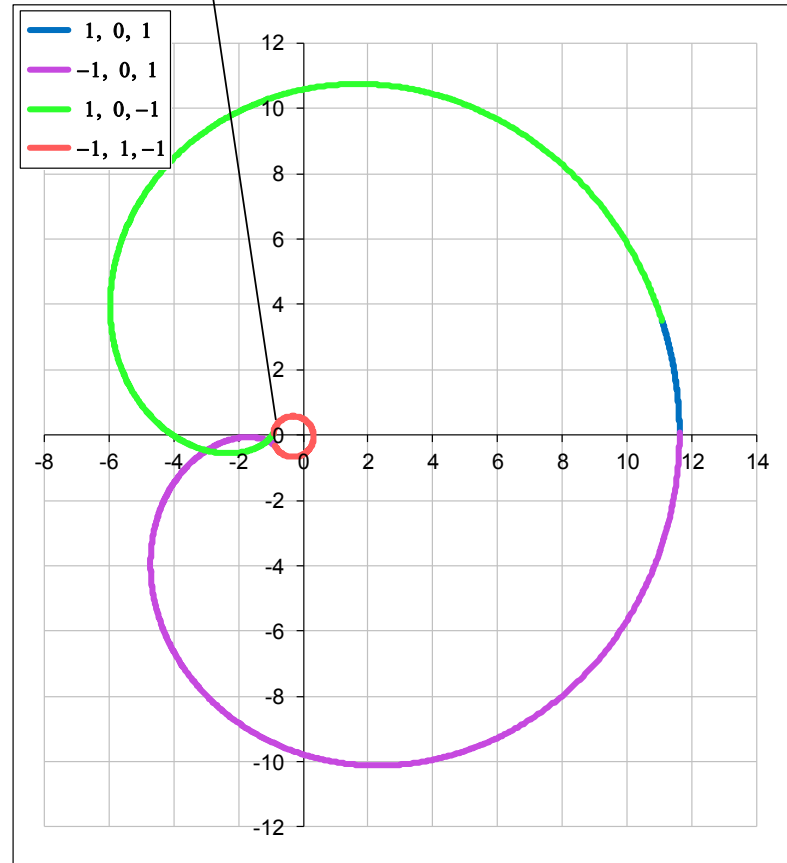
Without loss of generality, we assume that the initial instant and the initial phase vector are zero.

# Violation of simple connectedness of the reachable set



The plane of cross-section corresponds to  $\varphi = 0$

*This domain does not belong to the  $\varphi$ -section of the reachable set*



$\varphi$ -section of the reachable set  
for  $\varphi = 0.1\pi$  and  $t_f = 3.7\pi$

## Slide 5

From the results of numerical constructions, we know that some  $\varphi$ -sections may be non-simply connected. The figure on the right shows an example of such a  $\varphi$ -section. Here, the central area does not belong to the  $\varphi$ -section. A three-dimensional reachable set can also be non-simply connected. The corresponding example is shown in the left figure.

# Pontryagin Maximum Principle

It is known [Lee, E.B., Markus L.] that controls that carry a system onto the reachable set boundary satisfy the PMP.

$$\begin{cases} \dot{x} = \cos\varphi, \\ \dot{y} = \sin\varphi, \\ \dot{\varphi} = u; \end{cases} \quad \begin{array}{l} \text{dynamic description} \\ \text{of Dubins car} \end{array}$$

$$u \in [u_1, u_2], \quad u_1 = -1, \quad u_2 = 1$$

Reachable set at the instant  $t_f$ :

$$G(t_f) = \bigcup_{u(\cdot)} \begin{pmatrix} x(t_f) \\ y(t_f) \\ \varphi(t_f) \end{pmatrix}$$

Let  $u^*(\cdot)$  be some admissible control and  $(x^*(\cdot), y^*(\cdot), \varphi^*(\cdot))^T$  be the corresponding motion of Dubins car on the interval  $[t_0, t_f]$   
 Differential equations of the adjoint system :

$$\begin{cases} \dot{\psi}_1 = 0, \\ \dot{\psi}_2 = 0, \\ \dot{\psi}_3 = \psi_1 \sin\varphi^* - \psi_2 \cos\varphi^*. \end{cases}$$

We have  $\psi_1^*(\cdot) = \text{const}$ ,  $\psi_2^*(\cdot) = \text{const}$ .

## Slide 6

In the book by E.B. Lee and L. Markus, a theorem is formulated and proved that any open-loop control and its corresponding motion leading to the boundary of the reachable set satisfy the Pontryagin maximum principle. The type of conjugate system for the Dubins model is very simple.

# Pontryagin Maximum Condition

The PMP means that a nonzero solution  $(\psi_1^*(\cdot), \psi_2^*(\cdot), \psi_3^*(\cdot))^T$  of the adjoint system exists, for which almost everywhere (a.e.) on the interval  $[t_0, t_f]$ , the following condition is satisfied :

$$\psi_1^*(t)\cos\varphi^*(t) + \psi_2^*(t)\cos\varphi^*(t) + \psi_3^*(t)u^*(t) = \max_{u \in [u_1, u_2]} \left[ \psi_1^*(t)\cos\varphi^*(t) + \psi_2^*(t)\cos\varphi^*(t) + \psi_3^*(t)u \right]$$

$$\Rightarrow \psi_3^*(t)u^*(t) = \max_{u \in [u_1, u_2]} \left[ \psi_3^*(t)u \right], \text{ a.e. } t \in [t_0, t_f]$$

1. If  $\psi_1^* = 0$  and  $\psi_2^* = 0$ , then  $\psi_3^*(\cdot) = \text{const} \neq 0$  on the interval  $[t_0, t_f]$ .

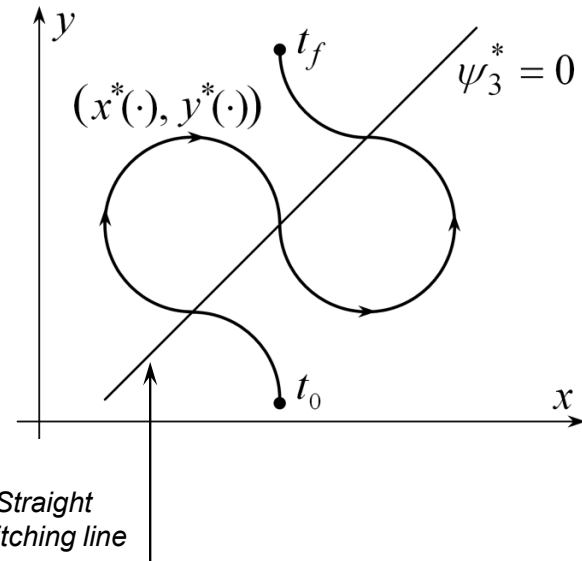
Therefore, we have a.e.  $u^*(t) = u_1$  or  $u^*(t) = u_2$ .

2. Let at least one of the numbers  $\psi_1^*$  and  $\psi_2^*$  is non-zero. Using the equations of dynamics and adjoint system equations, one can write

$$\psi_3^*(t) = \psi_1^*y^*(t) - \psi_2^*x^*(t) + C.$$

Therefore,  $\psi_3^*(t) = 0$  iff the point  $(x^*(t), y^*(t))^T$  of the geometric position at the instant  $t$  obeys the straight line equation

$$\psi_1^*y - \psi_2^*x + C = 0.$$



## Slide 7

Here, we write out the formula of the maximum principle, from which it follows that the control  $u^*(\cdot)$  leading to the boundary is determined at each instant  $t$  by the sign of the third component  $\psi_3^*(t)$  of the vector  $\psi^*(t)$  of the conjugate system. If the control  $u^*(\cdot)$  has two or more switches, then a switching line occurs. Note that straight switching line is not universal. For each motion leading to the boundary, the switching line is different.

The facts noted on this and previous slides are the simplest. They directly follow from the relations for the Pontryagin maximum principle. These relations also allow us to talk about a finite number of switches for each piecewise-constant control leading onto the boundary of the reachable set.

# Controls generating the boundary of three-dimensional reachable set

Theorem. Any boundary point of the reachable set for system

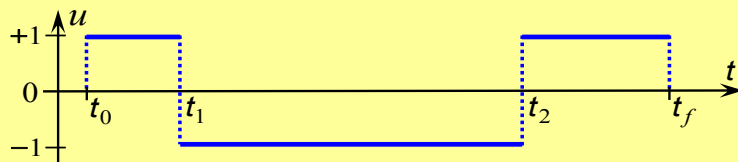
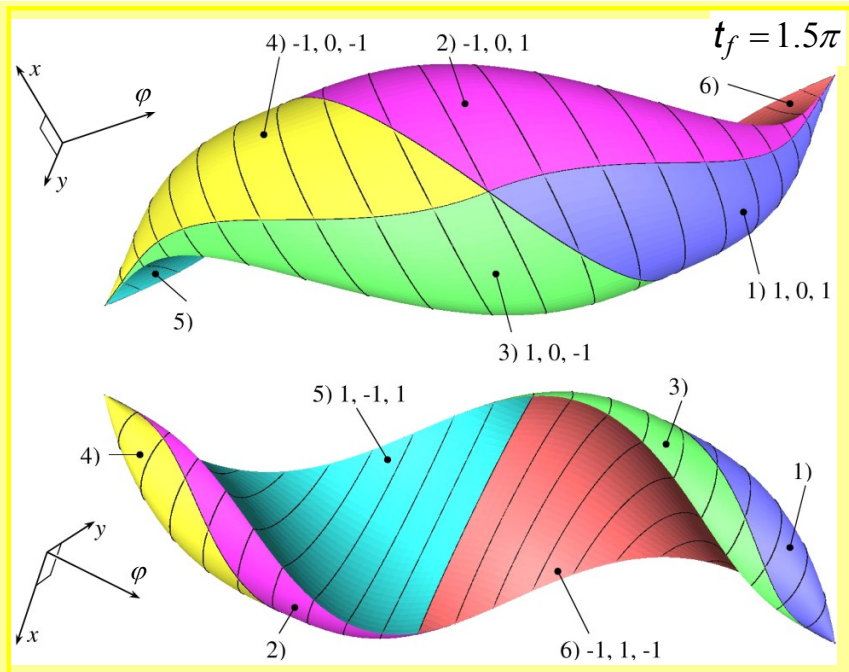
$$\dot{x} = \cos \varphi, \quad \dot{y} = \sin \varphi, \quad \dot{\varphi} = u; \quad |u| \leq 1$$

can be reached by means of a piecewise-constant control with no greater than two switching instants. In the case of two switchings, it is sufficient to consider 6 sequences of the control values, namely,

- 1)  $+1, 0, +1$ ; 2)  $-1, 0, +1$ ; 3)  $+1, 0, -1$ ;  
 4)  $-1, 0, -1$ ; 5)  $+1, -1, +1$ ; 6)  $-1, +1, -1$ .

Note: in the cases 5), 6), we can restrict by the motions that satisfy the inequality (Lemma 2)

$$(t_1 - t_0) + (t_f - t_2) \leq (t_2 - t_1)$$



Patsko V.S., Pyatko S.G., Fedotov A.A. (2003) Three-dimensional reachability set for a nonlinear control system. Journal of Computer and Systems Sciences International. Vol. 42, No. 3, pp. 320–328

Dubins L.E. (1957) On curves of minimal length with a constraint on average curvature and with prescribed initial and terminal positions and tangents. American J. Math. Vol. 79, no. 3. P. 497–516.

## Slide 8

On this slide, we present the formulation of our theorem from the paper of 2003, which determines the controls leading to the boundary of the reachable set *at the instant* for the Dubins car. These six types coincide with the controls indicated in the paper by L.Dubins related to the time-optimal problem. The difference lies in an additional condition that must be satisfied for controls of types 5) and 6). This condition means that the duration of the average interval of the control constancy must not be less than the total duration of the first and third intervals.

In our previous papers, we used this theorem to numerically construct the boundary of the reachable set. Since motions are explicitly integrated due to each of the six types of controls, now we use it as a basis for an analytical study of  $\varphi$ -sections of the three-dimensional reachable set.

# Classification of $\varphi$ -sections of three-dimensional reachable set

- I.  $0 \leq \varphi < t_f, \quad t_f < 4\pi - \varphi, \quad t_f < 3\pi + 2 \cos(\varphi/2).$
- II.  $0 \leq \varphi < \pi, \quad t_f < 4\pi - \varphi, \quad t_f \geq 3\pi + 2 \cos(\varphi/2).$
- III.  $0 \leq \varphi < 2\pi, \quad t_f \geq 4\pi - \varphi.$
- IV.  $2\pi \leq \varphi < t_f.$
- V.  $\varphi = t_f.$

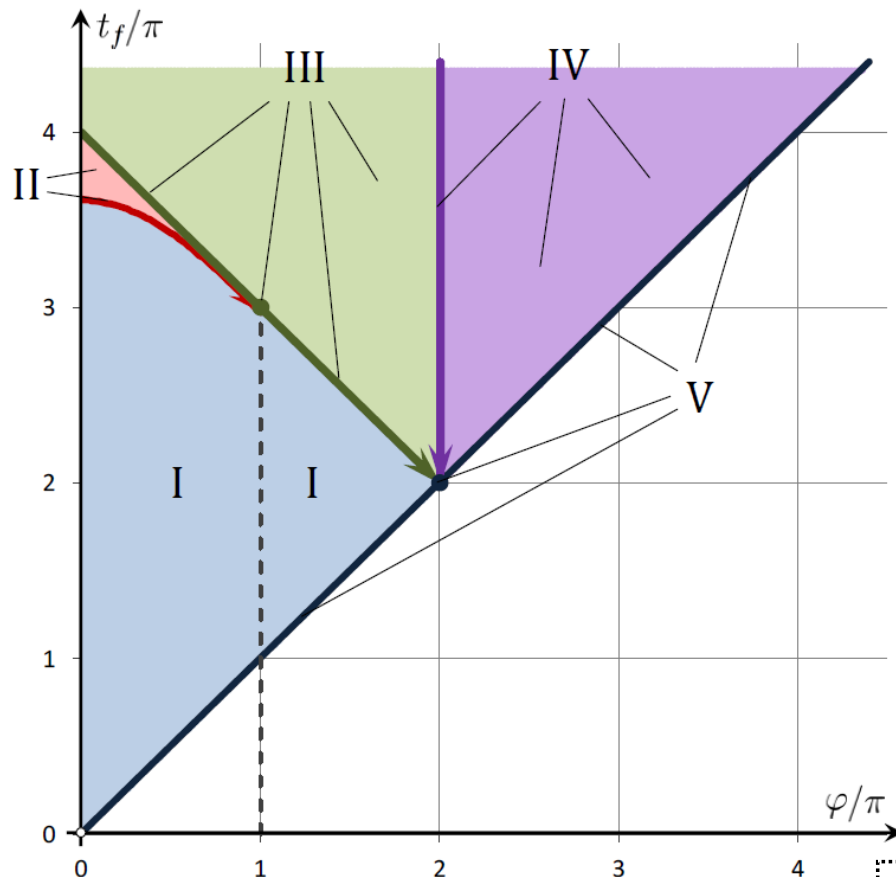
*The symmetry property  
to cover the case  $\varphi < 0$ :*

*if*  $u_*(t) = -u^*(t),$

*then*  $x_*(t_f) = x^*(t_f),$

$$y_*(t_f) = -y^*(t_f),$$

$$\varphi_*(t_f) = -\varphi^*(t_f).$$



## Slide 9

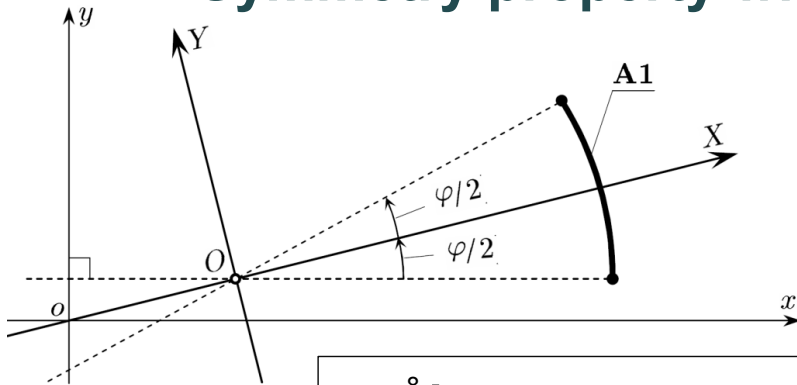
Up to this slide there was an introductory part of our report. Now, we turn to the presentation of new results. On the plane  $\varphi$  and  $t_f$ , we distinguish five sets, for each of which the structure of  $\varphi$ -sections is the same. The classification is shown for non-negative values  $\varphi$ . Specifics of the kinematic description of the Dubins car is revealed in the symmetry of the system motions when the sign of the control  $u(\cdot)$  is changed. Therefore, for the negative values  $\varphi$ , we obtain a picture of the classification that is symmetric to shown one with respect to the vertical axis.

The simplest case in the classification is number V. Here, each  $\varphi$ -section degenerates into a point.

Next, we turn to the consideration of cases I–IV.

# Auxiliary coordinate system $X, Y$ .

## Symmetry property with respect to the axis $X$



$$\varphi = \pi/4$$

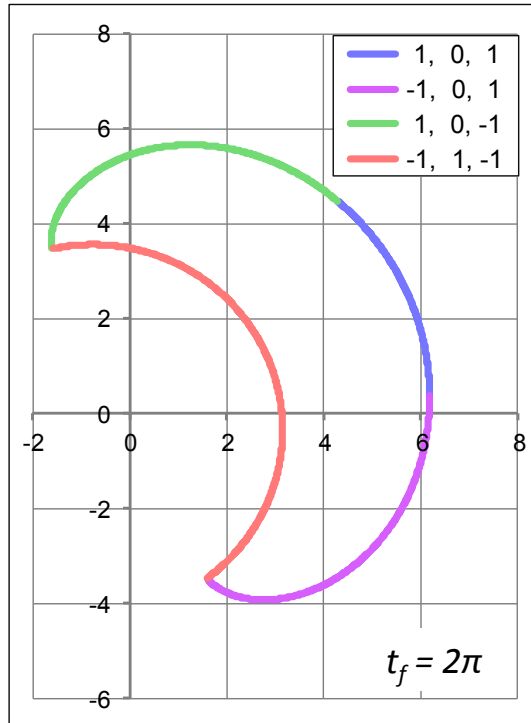
four types of curves :

**A1 : +1, 0, +1**

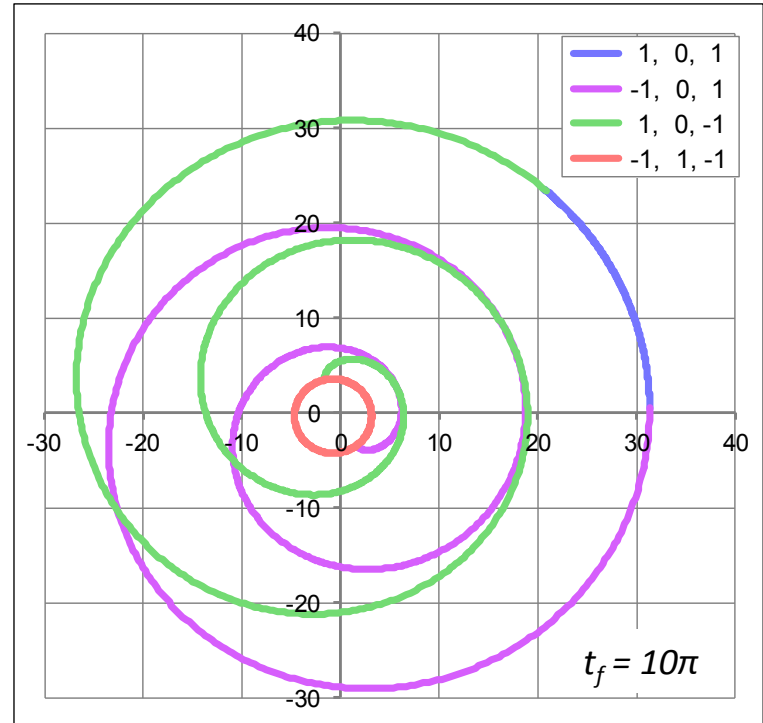
**A2 : -1, 0, +1**

**A3 : +1, 0, -1**

**A6 : -1, +1, -1**



For any  $t_f$  and  $\varphi \geq 0$ ,  $\varphi$ -section is symmetric with respect to the axis  $X$  of the auxiliary coordinate system  $X, Y$ . The axis  $X$  passes through the origin of the original system  $x, y$ .



## Slide 10

If  $\varphi \geq 0$ , then it is enough to take only four types of controls to describe the boundary of the reachable set: 1), 2), 3), and 6). With a fixed  $\varphi$ , each of them determines a one-parameter curve on the plane of geometric coordinates  $x, y$ . The corresponding curves are denoted as A1, A2, A3, and A6. Taking these curves in the sequence A1, A3, A6, and A2, we obtain a continuous closed curve that contains the boundary of the  $\varphi$ -section. Examples are shown at the bottom of the slide. For small values  $t_f$ , we have a closed curve without self-intersections (fig. on the left). As  $t_f$  increases, the closed curve under consideration becomes more complicated and the number of its self-intersections grows (fig. on the right). In this case, the problem of selecting segments of curves lying on the boundary of the  $\varphi$ -section becomes much more complicated.

Analyzing the introduced closed curve, we are convinced of its symmetry with respect to the axis  $X$  of some auxiliary coordinate system  $X, Y$  (upper part of the slide). The auxiliary coordinate system depends only on the value  $\varphi$ . The axis  $X$  passes through the origin of the original coordinate system.

Further analysis will use the formulas for writing curves A1, A2, A3, and A6 in the auxiliary coordinate system.

# The curves A2 and A3 are involutes of circles

$$s_2 = -t_1 \quad s_2 \in [-\theta, 0] \quad \theta = (t_f - \varphi)/2$$

$$s_3 = t_1 - \varphi \quad s_3 \in [0, \theta]$$

$$A2(s_2) = \begin{pmatrix} X_{U2}(s_2) \\ Y_{U2}(s_2) \end{pmatrix} = 2(\theta + s_2) \begin{pmatrix} \cos(s_2 - \frac{\varphi}{2}) \\ \sin(s_2 - \frac{\varphi}{2}) \end{pmatrix} - 4\sin\left(\frac{s_2}{2}\right) \begin{pmatrix} \cos\left(\frac{s_2}{2} - \frac{\varphi}{2}\right) \\ \sin\left(\frac{s_2}{2} - \frac{\varphi}{2}\right) \end{pmatrix}$$

$$A3(s_3) = \begin{pmatrix} X_{U3}(s_3) \\ Y_{U3}(s_3) \end{pmatrix} = 2(\theta - s_3) \begin{pmatrix} \cos(s_3 + \frac{\varphi}{2}) \\ \sin(s_3 + \frac{\varphi}{2}) \end{pmatrix} + 4\sin\left(\frac{s_3}{2}\right) \begin{pmatrix} \cos\left(\frac{s_3}{2} + \frac{\varphi}{2}\right) \\ \sin\left(\frac{s_3}{2} + \frac{\varphi}{2}\right) \end{pmatrix}$$

After trigonometric transformations, we obtain a parametric representation of each of the curves A2 and A3 in the form of an involute of a circle:

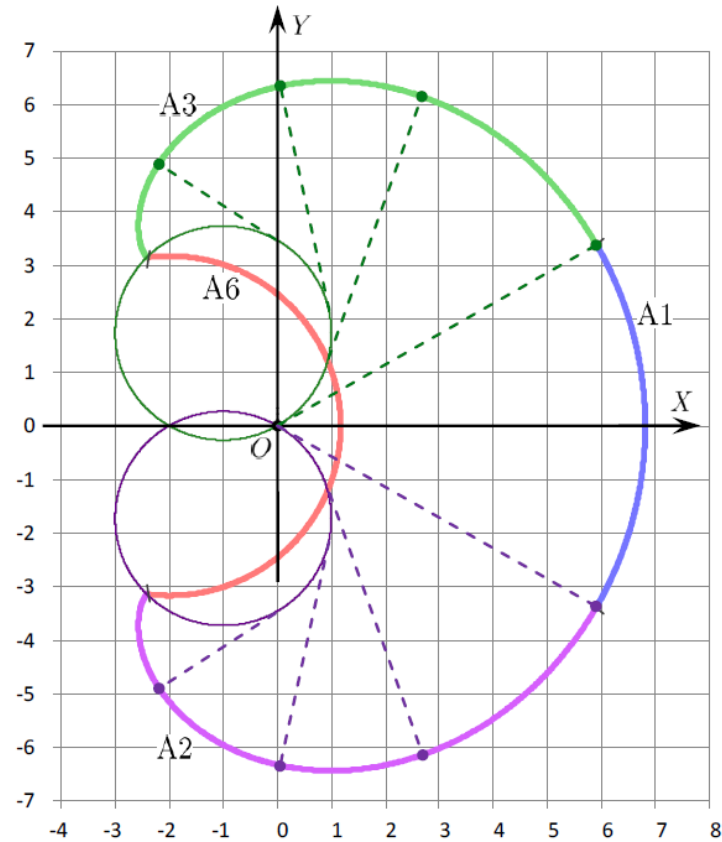
$$X(\tau) = r \cos \tau + r\tau \sin \tau,$$

$$Y(\tau) = r \sin \tau + r\tau \cos \tau.$$

Here,  $r$  is a base circle radius,  $\tau$  is a parameter (the angle of rotation of the generating straight line).

For curve A2, we have  $r = 2$ ,  $\tau = \theta + s_2$ , the center of base curve is  $2(-\sin(\varphi/2), -\cos(\varphi/2))^T$ .

For curve A3:  $r = 2$ ,  $\tau = \theta - s_3$ , the center of base curve is  $2(-\sin(\varphi/2), \cos(\varphi/2))^T$ .



$$t_f = 2.5\pi \quad \varphi = \pi/3$$

Dashed lines are not trajectories

## Slide 11

Here, at the top of the slide, formulas for parametric representation of the curves A2 and A3 in the auxiliary coordinate system are given. The curve A2 is determined with the help of the parameter  $s_2$ , and the curve A3 is given by the parameter  $s_3$ . Using trigonometric transformations, each of these two curves can be written in the standard form corresponding to the involute of the circle. In both cases, the radius of the base circle equals 2. However, the centers of these base circles, generally speaking, do not coincide.

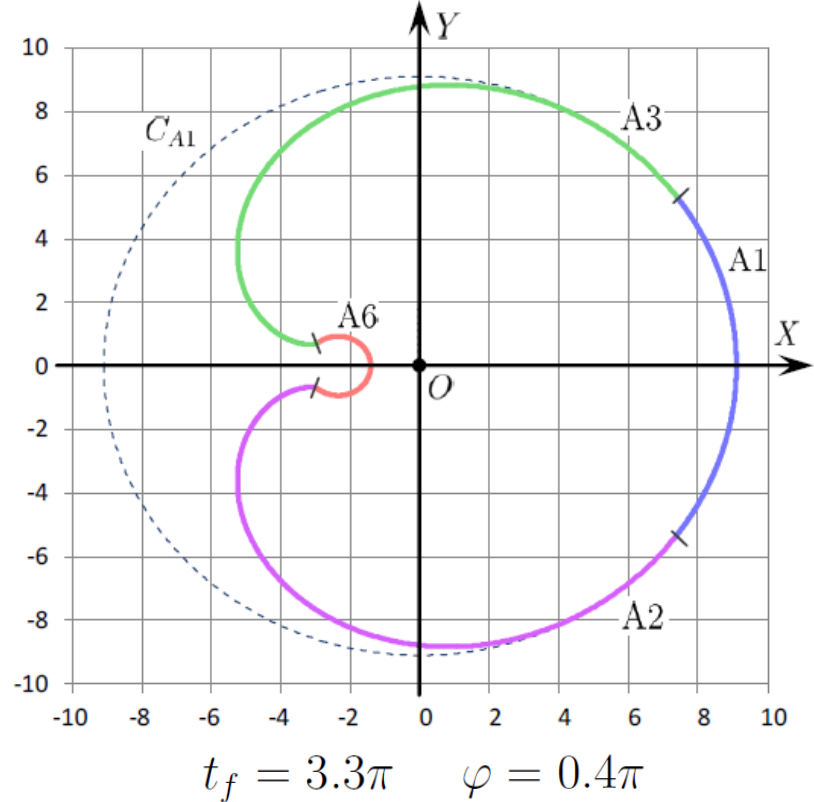
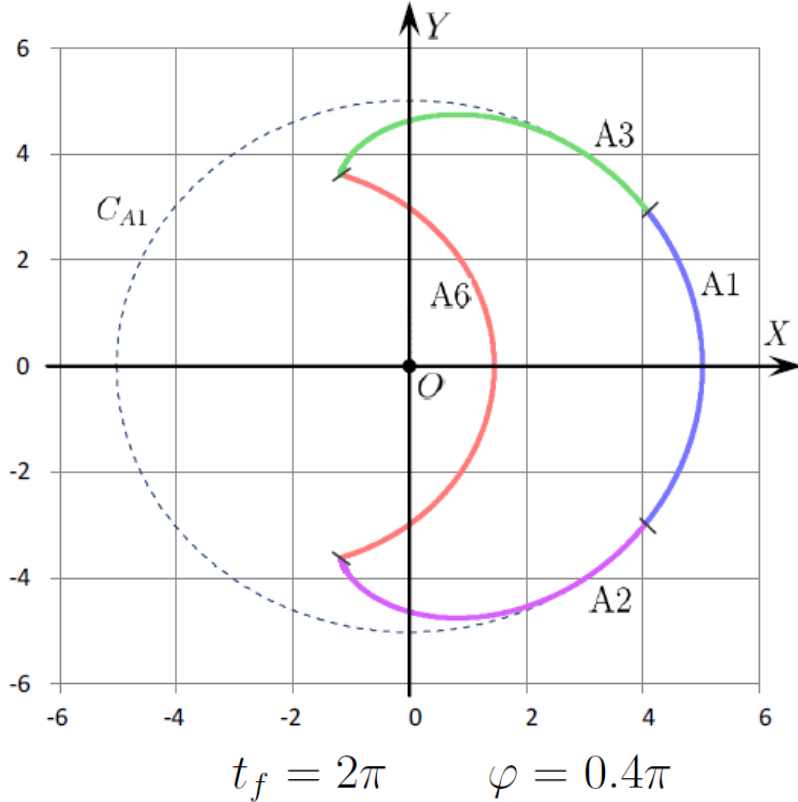
In the figure on the right, the involutes A2 and A3 are shown together with their base circles and with generating straight lines for the values  $t_f = 2.5\pi$  and  $\varphi = \pi/3$ . Generating straight lines are shown by dashed lines. In general, each generating curve (it consists of the base circle arc and the generating straight line) is not an extreme trajectory satisfying the Pontryagin maximum principle. We just interpret the curves A2 and A3 as the circle involutes in order to justify the geometric properties of these curves that we need. This is the difference from the above-considered projection of the three-dimensional reachable set onto the plane  $x, y$ .

Note that the curves A1 and A6 are always arcs of circles.

Thus, the boundary of any  $\varphi$ -section consists of some arcs of circles and some parts of involutes.

For the values  $t_f$  and  $\varphi$  indicated in the figure caption, the boundary of the  $\varphi$ -section includes the curves A1, A3, A6, and A2 entirely.

# View of $\varphi$ -sections for case I



The case I with an additional restriction  $t_f \leq 2\pi$  was considered in the paper

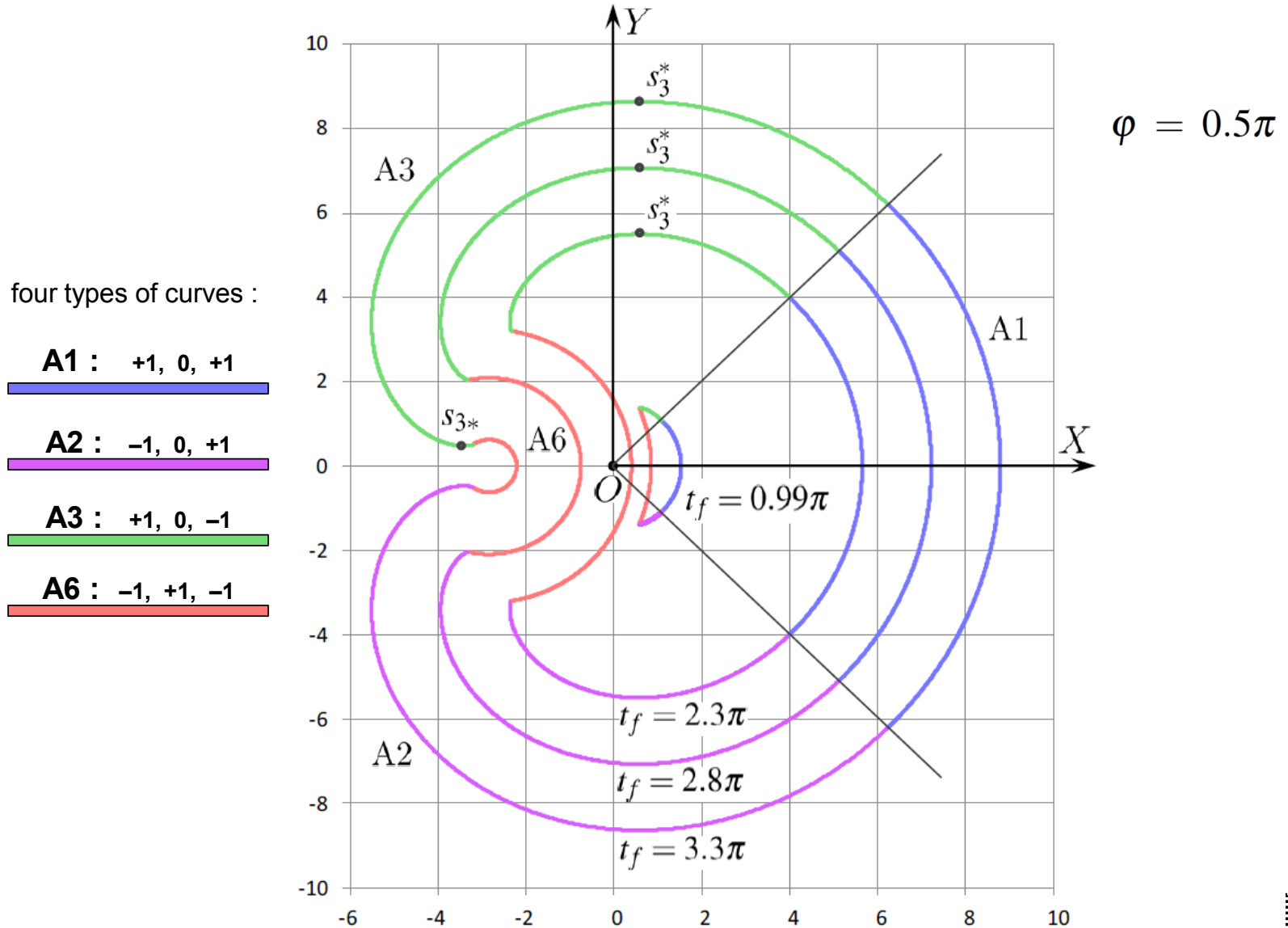
Patsko V.S., Fedotov A.A. (2020) Analytic description of a reachable set for the Dubins car. Trudy Instituta Matematiki i Mekhaniki URO RAN, vol. 26, no. 1, pp. 182–197 (in Russian).

## Slide 12

On this slide, we show the view of the  $\varphi$ -section boundary for the case I. The value  $\varphi$  is the same for both figures. For fig. on the left, the value  $t_f$  is less than for fig. on the right. The case I is characterized precisely by the fact that the boundary of the  $\varphi$ -section coincides with the closed curve formed by the sequentially connected curves A1, A3, A6, and A2. In the case I, the curves A2, A3, A6 are non-degenerate, and the curve A1 degenerates only when  $\varphi = 0$ .

The case I with the additional restriction  $t_f \leq 2\pi$  was considered in our paper of 2020.

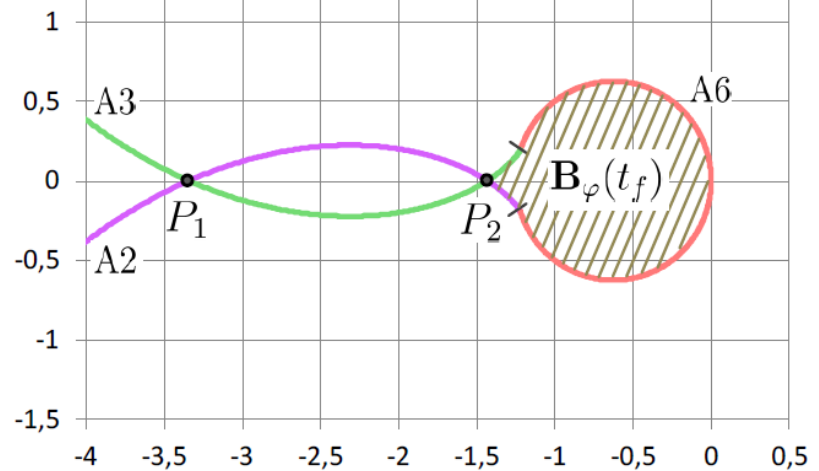
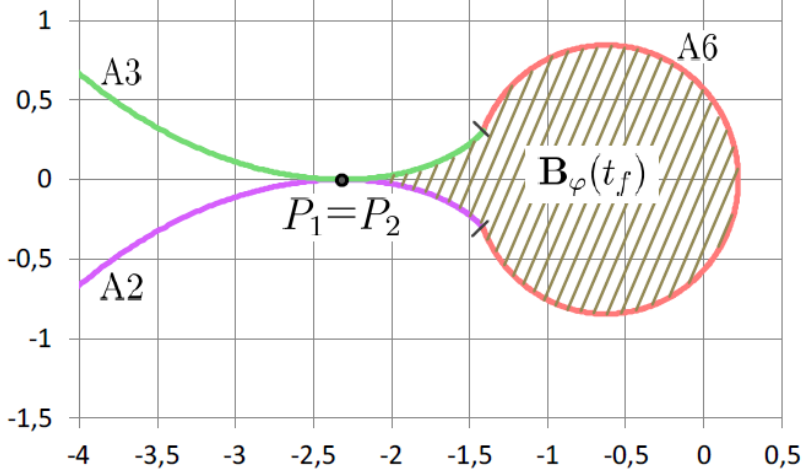
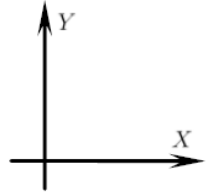
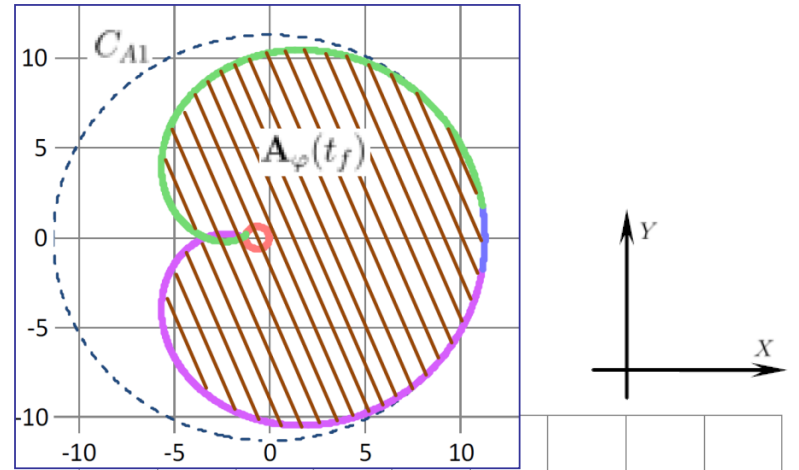
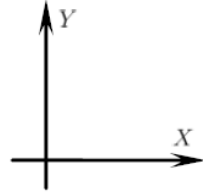
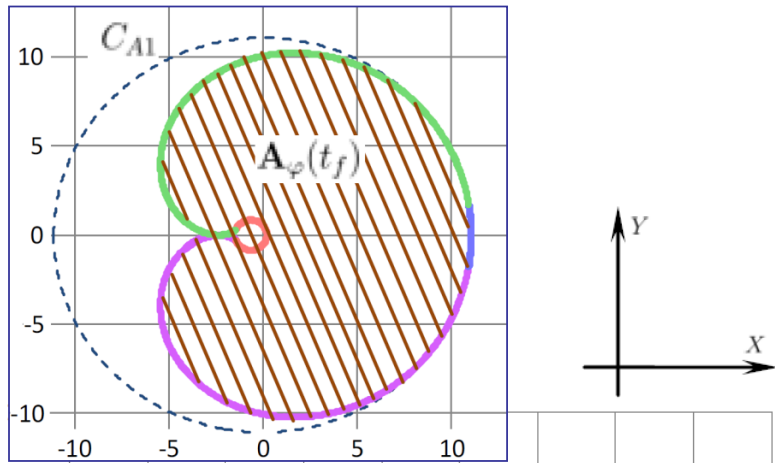
# Evolution of $\varphi$ -section in time for case I ( $\varphi$ is fixed)



## Slide 13

Here, for the case I, the evolution of the  $\varphi$ -section boundary is shown with the increasing instant  $t_f$  for the fixed value  $\varphi = 0.5\pi$ . It can be seen that the curves A1 are concentric arcs of circles with the same angular span. The curves A6 are also arcs of concentric circles. The curves A2 and A3 (involutives) join smoothly with the curve A1, but their joining with the curve A6 is not smooth.

# View of $\varphi$ -sections for case II



$$t_f = 3\pi + 2 \cos(0.05\pi), \quad \varphi = 0.1\pi$$

$$t_f = 3.7\pi, \quad \varphi = 0.1\pi$$

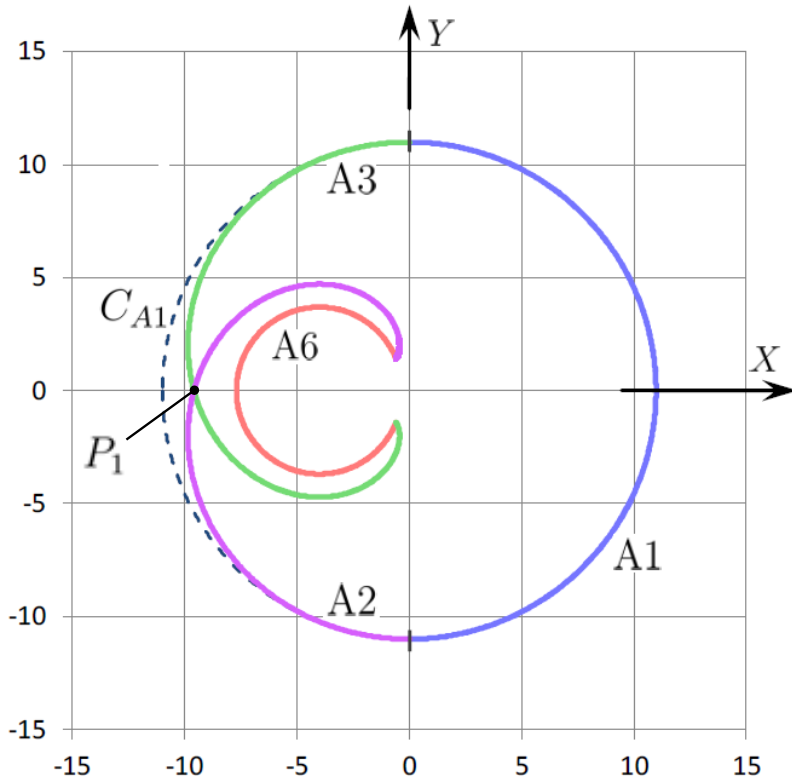
$$G_\varphi(t_f) = \mathbf{A}_\varphi(t_f) \setminus \text{int} \mathbf{B}_\varphi(t_f)$$

## Slide 14

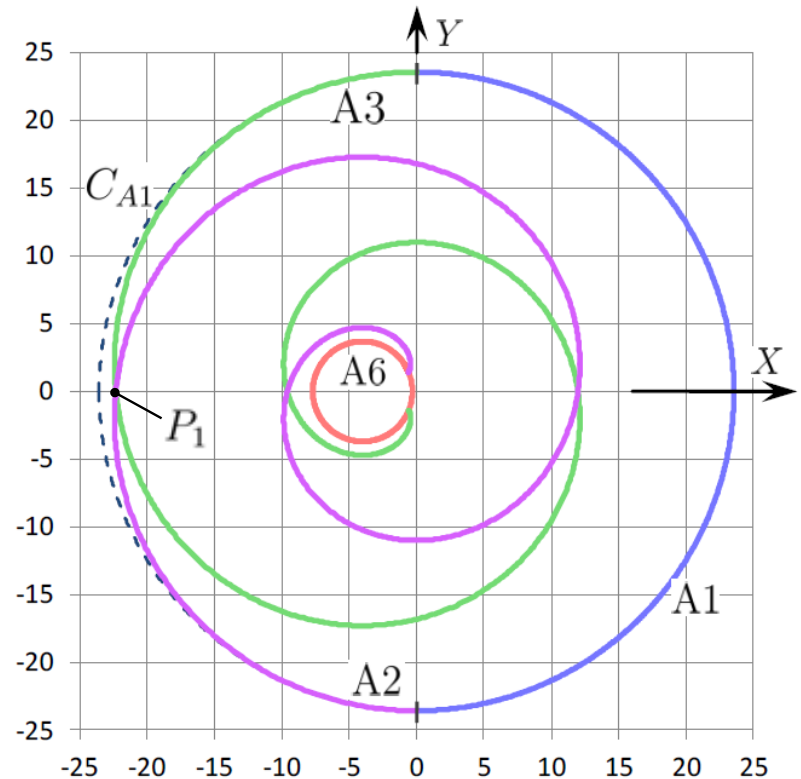
The main feature of  $\varphi$ -sections in the case II is that they are not simply connected. The  $\varphi$ -sections considered here are given by the outer and inner boundaries. This slide represents two examples of  $\varphi$ -sections for a fixed value  $\varphi = 0.1\pi$ . In the upper part of the slide, the sets  $G_\varphi(t_f)$  are shown in their entirety, and in the lower part their enlarged fragments are given showing the peculiarity arising in the case II. The value  $t_f$  for the left figure corresponds to the first time instant when the curves A2 and A3 touch (touch point  $P_1=P_2$ ). In the right figure (for a larger value  $t_f$ ) the curves A2, A3 are already intersected at two different points  $P_1$  and  $P_2$ .

The feature of the case II is realized in the appearance of a set  $B_\varphi(t_f)$  whose interior does not belong to the  $\varphi$ -section. The boundary of the "hole"  $B_\varphi(t_f)$  (the inner boundary of the  $\varphi$ -section) is composed of the curve A6 and adjacent parts of the curves A2 and A3 to the point  $P_2$ . The outer boundary is formed by the curve A1 and adjacent parts of the curves A2, A3, taken up to the point  $P_1$ .

# View of $\varphi$ -sections for case III (non-degenerate subcase: $t_f > 4\pi - \varphi$ )



$$t_f = 4.5\pi, \quad \varphi = \pi$$



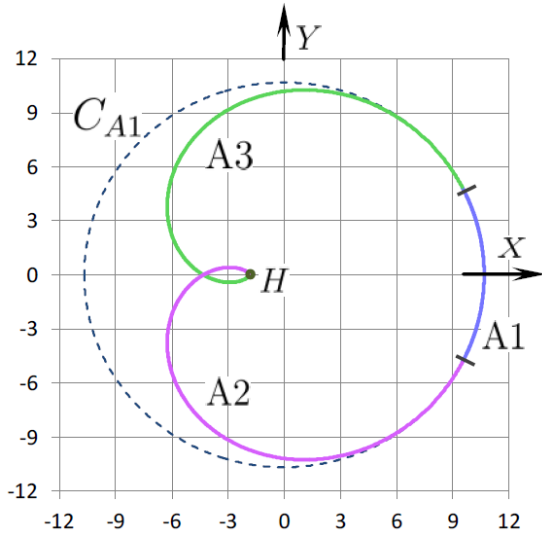
$$t_f = 8.5\pi, \quad \varphi = \pi$$

The boundary of  $\varphi$ -section in this case is formed by the curve A1 and parts of the curves (the involutes) A2 and A3 up to the point of their first intersection

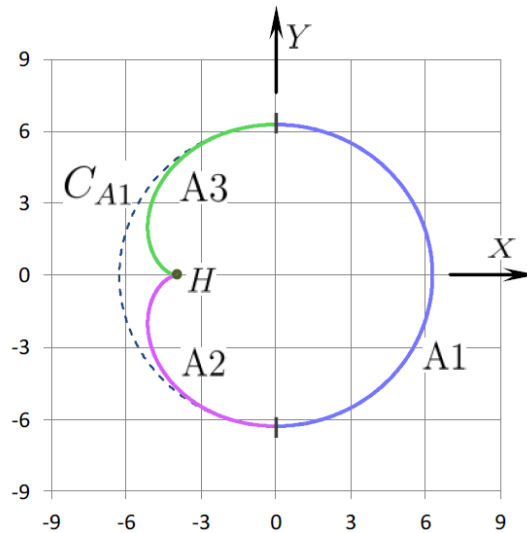
## Slide 15

This slide shows examples of  $\varphi$ -sections for the case III under the condition  $t_f > 4\pi - \varphi$  (non-degenerate subcase). Here, the curve A6 and some parts of the curves A2, A3 are located in the interior of the  $\varphi$ -section. The set  $G_\varphi$  is simply connected. Its boundary is formed by the curve A1 and parts of the curves A2, A3 taken up to the point  $P_1$  of their intersection. For large values  $t_f$ , the curves A2 and A3 can intersect many times (fig. on the right).

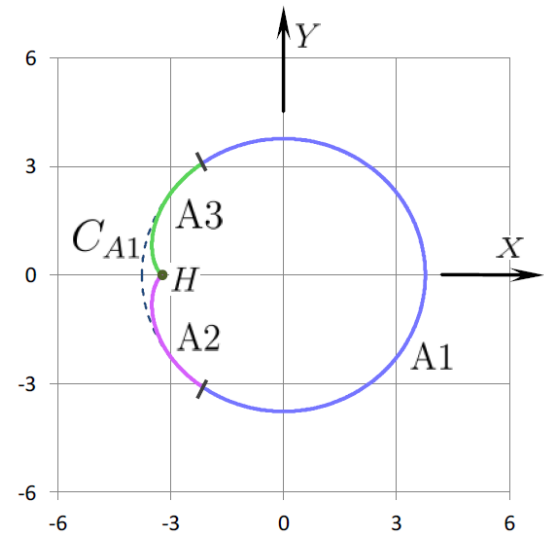
# View of $\varphi$ -sections for case III (degenerate subcase: $t_f = 4\pi - \varphi$ )



$$\varphi = 0.3\pi, t_f = 3.7\pi$$



$$\varphi = 1.0\pi, t_f = 3.0\pi$$



$$\varphi = 1.4\pi, t_f = 2.6\pi$$

Curves A1, A2, A3 are shown in full. Curve A6 degenerates into point H.  
In the last two pictures, the first intersection point of the curves A2 and A3 coincides with the point H.

The boundary of  $\varphi$ -section in this case is formed by the curve A1 and parts of the curves (the involutes) A2 and A3 up to the point of their first intersection.

## Slide 16

This subcase of the case III borders with case II for  $\varphi < \pi$  and with case I for  $\varphi \geq \pi$  (see classification on slide 9). For both conditions, the curve A6 consists of one point.

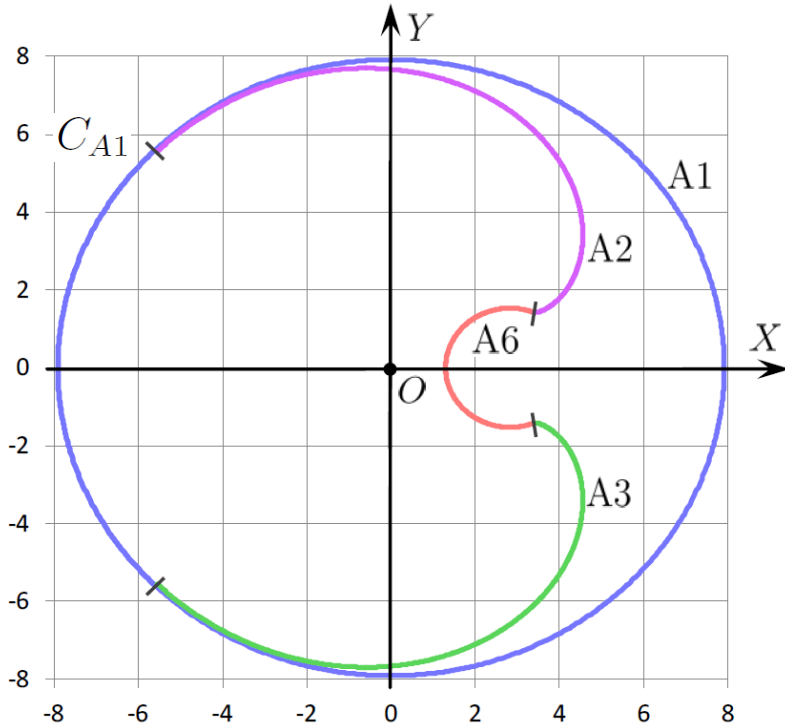
The left figure shows an example for  $\varphi < \pi$ . Here we have the set  $B_\varphi(t_f)$  (is introduced for case II) degenerating into the point  $H$ . The boundary of the  $\varphi$ -section consists of the arc A1 and the arcs A2 and A3 up to the point of their first intersection.

On the middle and right figures, the examples are shown for  $\varphi \geq \pi$ . Here, too, the curves A2 and A3 after hitting the point H have no continuation. We obtain the boundary of the  $\varphi$ -section as sequential connecting the curves A1, A3, and A2.

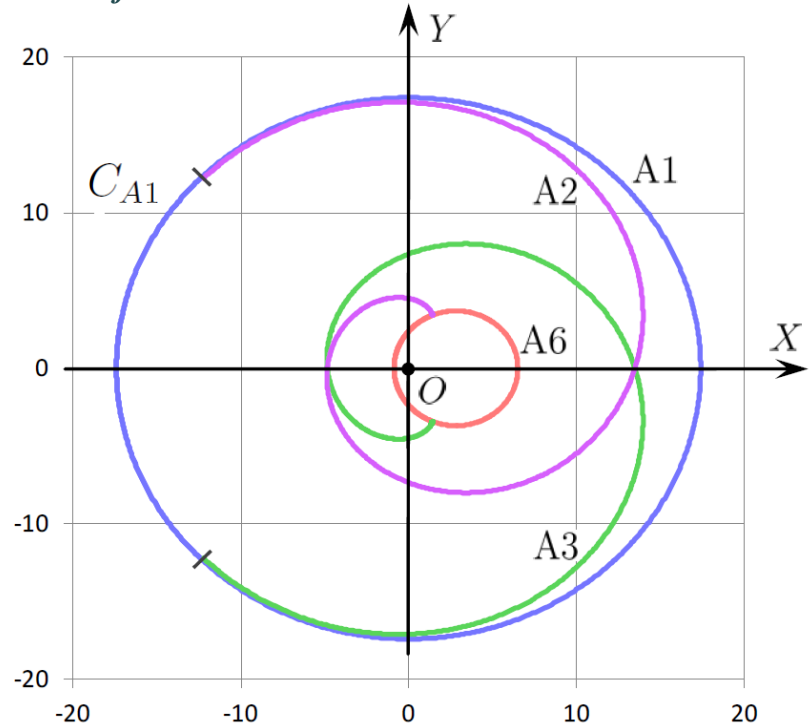
In general, the boundary of the  $\varphi$ -section is described using three curves (as in the non-degenerate subcase of the case III).

# View of $\varphi$ -sections for case IV

$$(2\pi \leq \varphi < t_f)$$



$$t_f = 5\pi, \quad \varphi = 2.5\pi$$



$$t_f = 8\pi, \quad \varphi = 2.5\pi$$

The curve A1 is a circle with an “overlap” (with a scope greater than  $2\pi$ ).

The set  $G_\varphi(t_f)$  is the circle  $C_{A1}$ .

## Slide 17

The case IV is determined by the condition  $2\pi \leq \varphi < t_f$ . Here, the curve A1 is a circle (a circumference) with an “overlap”. This circle is the boundary of the  $\varphi$ -section. The center of the circle coincides with the origin of the auxiliary coordinate system, and the radius is equal to  $t_f - \varphi$ . The curve A6 as a whole and the curves A2 and A3, except the points of their joining with the curve A1, lie in the interior of the set  $G_\varphi(t_f)$  and do not participate in the formation of its boundary.

# Summary

An analytical description of the boundary of two-dimensional  $\varphi$ -sections of the three-dimensional reachable set for Dubins car is obtained including the case of not simply connected  $\varphi$ -sections.

The boundary of each  $\varphi$ -section is formed by means of arcs of circles and parts of involutes.

A classification of possible variants of  $\varphi$ -section structure is introduced.

The results obtained can be used in solving various control problems.

## Slide 18

The paper investigates the structure of cross sections by angular coordinate ( $\varphi$ -sections) of three-dimensional reachable set “at instant” for the Dubins car. Curves lying on the boundary of  $\varphi$ -sections are analyzed. Their analytical description is obtained.

# Future

An asymmetric case of restrictions on left and right turns will be considered.  
We plan to prove that its study reduces to the symmetric case.

$$\dot{x} = \cos \varphi,$$

$$\dot{y} = \sin \varphi,$$

$$\dot{\varphi} = u;$$

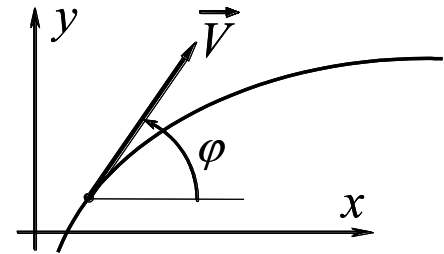
$$u \in [u_1, u_2]$$

$$u_1 = -1, \quad u_2 = 1$$

(symmetric case)

$$u_1 < 0 < u_2$$

(asymmetric case with two-sided turns)



$$\varphi \in (-\infty, +\infty)$$

Let us need to find  $\varphi$ -section  $G_\varphi(t_f)$  for some values  $t_f$  and  $\varphi$  in the asymmetric case.

We introduce the instant  $t_f^*$  by the formula  $t_f^* = \frac{2u_1(\varphi - t_f u_2)}{u_2 - u_1} + \varphi$ .

Given the same value  $\varphi$ , we consider the  $\varphi$ -section  $G_\varphi^*(t_f^*)$  for the symmetric case. In the auxiliary coordinate system (it depends only on  $\varphi$ ), we obtain the desired  $\varphi$ -section  $G_\varphi(t_f)$  using the linear transformation (with multiplication by the coefficient and the shift):

$$G_\varphi(t_f) = \frac{u_1 - u_2}{2u_1 u_2} G_\varphi^*(t_f^*) + 2 \sin\left(\frac{\varphi}{2}\right) \begin{pmatrix} \frac{1}{u_2} - 1 \\ 0 \end{pmatrix}.$$

## Slide 19

In our work for the controlled object "Dubins car", the case of symmetric control constraint is considered:  $u \in [-1, 1]$ . We plan to prove that the results obtained can also be used for any asymmetric constraint of the form  $u_1 \leq 0 \leq u_2$ . Namely, in the asymmetric case, for any  $t_f$  and  $\varphi$ , the desired  $\varphi$ -section can be obtained from the symmetric case by taking the same value  $\varphi$ , but some other value  $t_f^*$  instead of  $t_f$ .